

Geophysical Research Letters

RESEARCH LETTER

10.1029/2018GL081194

Special Section:

Bridging Weather and Climate: Subseasonal-to-Seasonal (S2S) Prediction

Key Points:

- Atmospheric river occurrence in the North Atlantic region differs during distinct low-frequency flow patterns, so-called weather regimes
- Blocking anticyclones during weather regimes deviates moisture transport around blocked regions and modulates atmospheric river occurrence
- The likelihood of extreme precipitation in Europe is altered during distinct weather regimes due to the modulation of atmospheric river landfall

Supporting Information:

- Supporting Information S1

Correspondence to:

J. T. Pasquier,
julie.pasquier@env.ethz.ch

Citation:

Pasquier, J. T., Pfahl, S., & Grams, C. M. (2019). Modulation of atmospheric river occurrence and associated precipitation extremes in the North Atlantic Region by European weather regimes. *Geophysical Research Letters*, *46*, 1014–1023. <https://doi.org/10.1029/2018GL081194>

Received 12 NOV 2018

Accepted 17 DEC 2018

Accepted article online 27 DEC 2018

Published online 19 JAN 2019

Modulation of Atmospheric River Occurrence and Associated Precipitation Extremes in the North Atlantic Region by European Weather Regimes

J. T. Pasquier¹ , S. Pfahl^{1,2} , and C. M. Grams^{1,3} 

¹Institute for Atmospheric and Climate Science, ETH Zurich, Zurich, Switzerland, ²Institute of Meteorology, Freie Universität Berlin, Berlin, Germany, ³Institute of Meteorology and Climate Research (IMK-TRO), Karlsruhe Institute of Technology, Karlsruhe, Germany

Abstract The variability of large-scale moisture transport by atmospheric rivers (AR) and its linkage to precipitation extremes in the North Atlantic-European region is studied. A weather regime approach is adopted to describe the variability of the large-scale circulation. Weather regimes modulate the climatologically mean westerly flow into Europe, in which ARs are commonly embedded. In cyclonic regimes, AR landfall is enhanced in wide parts of Iberia, Western Europe, the British Isles, and southern Scandinavia. In blocked regimes, ARs are deviated around the blocking anticyclone enhancing AR landfall at high latitudes or in the western Mediterranean and North Africa. The likelihood of precipitation extremes increases locally more than twofold in regions of enhanced AR occurrence during the different weather regimes. These results suggest that specific weather regimes establish favorable conditions for AR landfall in Europe. Therefore, accurate forecasts of weather regimes can give guidance for predicting also large-scale precipitation extremes.

Plain Language Summary Atmospheric rivers (ARs) are elongated bands of strong water vapor transport, which are embedded in the large-scale atmospheric circulation. ARs resemble rivers on land except that, instead of liquid water, ARs transport water vapor which is important for the formation of precipitation. The amount of water transported by an AR can be similar to the one of the largest rivers on land. These ARs frequently trigger precipitation extremes along the west coasts of the midlatitude continents. In this study, we investigate how the large-scale circulation influences AR's landfall location and subsequent precipitation extremes in Europe. To represent the natural variability of the westerly flow, we use seven typical persistent flow patterns over the North Atlantic-European region, called weather regimes (WRs). WRs characterized by a strong zonal flow enhance AR landfall in Iberia, Western Europe, the British Isles, and southern Scandinavia. WRs characterized by an anticyclone over Europe deviate ARs around the blocking anticyclone enhancing AR landfall at high latitudes or in the western Mediterranean and North Africa. The likelihood of precipitation extremes increases in regions of enhanced AR occurrence during the different WRs. Therefore, accurate WRs forecasts can give guidance for predicting also large-scale precipitation extremes in Europe.

1. Introduction

The major fraction of poleward moisture transport occurs in narrow filaments of strong water vapor transport in the lower troposphere, so-called atmospheric rivers (ARs; Zhu & Newell, 1998). ARs are frequently embedded within the warm sector of extratropical cyclones, in the low-level jet region just ahead of the cold front (e.g., Dacre et al., 2015; Gimeno et al., 2014; Neiman et al., 2008; Ralph et al., 2004, 2005). Due to their large amount of water vapor, ARs can cause precipitation and flooding when making landfall, especially if the moist air is forced to ascent in mountainous regions (Dettinger, 2011). It is expected that the increasing atmospheric moisture content in a warming atmosphere will enhance the intensity of ARs (Dettinger, 2011; Lavers et al., 2013; Warner et al., 2015). Therefore, and due to the severe socioeconomic impacts of the flooding and landslides already associated with ARs in present-day climate (Mastin et al., 2010; Neiman et al., 2011; Piaget et al., 2015), understanding mechanisms determining AR landfall is of utmost importance.

The impact of ARs on precipitation has been widely investigated in limited geographical regions and/or for short time periods. Most studies focused on AR's triggering precipitation in western North America (e.g.,

Dettinger et al., 2011; Guan et al., 2010; Neiman et al., 2008, 2011; Payne & Magnusdottir, 2014; Ralph et al., 2005, 2006; Rivera et al., 2014) and in Western Europe, for example, the UK (Champion et al., 2015; Lavers et al., 2011, 2012), Norway (Sodemann & Stohl, 2013; Stohl et al., 2008), or the Iberian Peninsula (Eiras-Barca et al., 2016; Ramos et al., 2015). Moreover, the relationship between ARs and precipitation was further established in coastal regions worldwide, for example, the Andes (Viale & Nuñez, 2011), Japan (Hirota et al., 2016), South Africa (Blamey et al., 2018), and Antarctica (Gorodetskaya et al., 2014). Even if ARs mostly impact coastal areas, they can penetrate and trigger precipitation farther inland as far as Poland, Germany (Lavers & Villarini, 2013; Piaget et al., 2015), or central Arizona (Neiman et al., 2013).

It has commonly been recognized that ARs are more frequent during the cold season due to the association between ARs and extratropical cyclones (Gimeno et al., 2014; Guan & Waliser, 2015), and several studies only focus on winter months (e.g., Brands et al., 2017; Lavers et al., 2011; Payne & Magnusdottir, 2014; Ralph et al., 2004; Rutz et al., 2014). Additionally, a majority of the literature assert that ARs cause more precipitation on land during the cold season because the moisture transport is stronger and air is closer to saturation (e.g., Champion et al., 2015; Eiras-Barca et al., 2016; Guan & Waliser, 2015; Lavers & Villarini, 2013; Neiman et al., 2008).

Moisture Conveyor Belts (Bao et al., 2006) and Tropical Moistures Exports (Knippertz & Wernli, 2010) are other flow concepts related to the tropospheric meridional transport of large amounts of water vapor. A particularity of these two flow concepts is the prerequisite to have a tropical moisture source. In contrary, a tropical origin is not required in the definition of ARs (Bao et al., 2006). In fact, both tropical moisture (Jankov et al., 2009; Neiman et al., 2008) and local moisture convergence in the extratropics (Bao et al., 2006; Dacre et al., 2015) were found to be important for the formation and maintenance of ARs.

The large-scale atmospheric flow influences AR occurrence and determines if and where ARs make landfall and possibly trigger precipitation (Guan & Waliser, 2015; Lavers & Villarini, 2013; Neiman et al., 2008; Payne & Magnusdottir, 2014; Rutz et al., 2014). The connection between ARs and precipitation in the North Atlantic-European region has been studied for different phases of the North Atlantic Oscillation (NAO). An enhanced influence of ARs on precipitation was found to occur over southern Europe during the negative phase of the NAO (Eiras-Barca et al., 2016; Lavers & Villarini, 2013) and over northern Europe during the positive phase of the NAO (Lavers & Villarini, 2013; Stohl et al., 2008). In contrast, Ramos et al. (2015) assess that the NAO pattern is not correlated with the number of ARs over the Iberian Peninsula. In addition, Lavers and Villarini (2013) showed that the latitude of AR landfall in Europe is strongly modulated by the prevailing large-scale mean sea level pressure pattern. Low-frequency weather regimes (WRs) provide a more detailed description of the large-scale circulation over the North Atlantic European region than the NAO and, in contrast to the NAO, describe the major part of variability on subseasonal (10–60 days) time scales (e.g., Grams et al., 2017; Zubieta et al., 2017).

WRs modulate the intensity and position of the midlatitude jet stream (e.g., Madonna et al., 2017) and accompanying cyclone activity. Thus, the large-scale flow pattern is different in the different WRs, which likely affects the occurrence of AR and heavy precipitation events (Lavers & Villarini, 2013; Santos et al., 2016; Yiou & Nogaj, 2004).

In this study, we use an extended definition of seven North Atlantic-European WRs (Grams et al., 2017) to investigate the modulation of AR activity due to variability of the large-scale circulation in the North Atlantic-European region. The study is organized as follows. First, we examine the autumn climatology of ARs in the North Atlantic-European region. In a second step, we investigate the modulation of AR occurrence during different low frequency WRs. Finally, we evaluate if this modulation influences also the likelihood of precipitation extremes (PEs) in Europe.

2. Data and Methods

2.1. Reanalysis Data

The European Centre for Medium-Range Weather Forecasts Interim Reanalysis (Dee et al., 2011) forms the data basis of this study and is used to detect ARs, WRs, and PEs. If not stated otherwise, we use global 6-hourly European Centre for Medium-Range Weather Forecasts Interim Reanalysis data interpolated on

a regular geographical grid at 1° horizontal resolution and the considered period is 1 January 1979 until 31 December 2014.

2.2. ARs

There is no generally accepted criterion or algorithm to identify ARs, and studies were completed using different criteria which were oriented along the specific aim of the study. A recent international collaborative effort within the Atmospheric River Tracking Method Intercomparison Project aims at understanding and quantifying the uncertainties in AR science based on different detection algorithms (Shields et al., 2018). Algorithms generally identify elongated objects of enhanced vertically integrated water vapor content (IWV) and/or vertically integrated vapor transport (IVT). Anomalous IWV and IVT related to AR can either be detected by absolute thresholds in these fields or relative thresholds with respect to a local climatology. Here we adopt a detection algorithm using absolute thresholds, as we aim to study the modulation of the actual moisture transport by the large-scale extratropical circulation that eventually leads to impactful precipitation events in Europe.

ARs are identified as two-dimensional objects with spatial extensions of at least 2,000 km in one direction. Every grid point within this object must fulfill the criteria that (1) the vertically integrated IWV is larger than 20 kg/m² and (2) the vertically IVT is larger than 250 kg·m⁻¹·s⁻¹. Furthermore, ARs are only identified northward of 20° N. These criteria and algorithm emerged from discussions in the AR research community (<https://eos.org/meeting-reports/setting-the-stage-for-a-global-science-of-atmospheric-rivers>), compare well with other methods, and are easily reproducible. Similar methods based on the same absolute thresholds have been used in earlier studies (e.g., Dettinger et al., 2011; Gershunov et al., 2017; Gimeno et al., 2014; Moore et al., 2012; Neiman et al., 2008; Ralph et al., 2004, 2006; Ralph & Dettinger, 2011; Rutz et al., 2014; and Shields et al., 2018 for an overview). AR frequencies are calculated by averaging the binary ARs field over the considered time period.

2.3. WRs

To characterize the large-scale flow situation, we employ a year-round definition of seven WRs previously introduced in the context of wind power (Grams et al., 2017) and maritime cold air outbreaks (Papritz & Grams, 2018). Seasonal WR definitions (e.g., Cassou, 2008; Ferranti et al., 2015; Michelangeli et al., 1995) struggle in identifying robust patterns in the transition seasons as these are characterized by both summer and winter regimes (cf. discussion in Supplement of Cassou, 2008). The extended seven WRs reflect the variability in large-scale flow patterns across all seasons, and thus also in autumn, which is the season of interest in this study. Consistent with earlier work, the WRs are obtained from a *k*-means clustering in the phase space spanned by the first seven empirical orthogonal functions (EOFs) of low-pass filtered, normalized 500-hPa geopotential height anomalies (Z500*) in the Euro-Atlantic sector (80°W–40°E, 30–90°N) available 6-hourly from 11 January 1979 to 31 December 2015 (Grams et al., 2017). Geopotential height anomalies are defined with respect to the 90-day running mean of the climatology for the respective date. In addition, WR life cycles are objectively identified based on the normalized projection of each 6-hourly Z500* into the cluster mean (see Grams et al., 2017) which allows us to filter out time steps that do not exhibit a well-established regime (“no regime,” about 31% of all days in autumn). Note that in contrast to the bimodal NAO or AO, which are typically derived from the first EOF explaining about 20–25% of the variance, WRs are based on the seven leading EOFs explaining about 75% of the variance and thus cover almost the full range of large-scale flow variability.

2.4. PEs and Cyclone Identification

The PE definition used in this work follows the method of Pfahl and Wernli (2012). At each grid point, PEs are defined as the 1% most extreme 6-hourly precipitation events per season using data from 1 January 1979 to 31 December 2015. This corresponds to the time steps when the precipitation exceeds the 99% local percentile. This method allows associating PE with atmospheric flow features in an event-based manner and on a grid point basis (Pfahl & Wernli, 2012).

Cyclones are identified from sea level pressure following an updated version of the method of Wernli and Schwierz (2006; see also Sprenger et al., 2017).

3. Results

The mean AR frequency in the North Atlantic region in autumn (September to November; Figure 1h) shows that the 500-hPa geopotential height field (Z500) is characterized by a climatological mean trough over the North American East Coast and a climatological mean ridge over the eastern North Atlantic and Western Europe (contours in Figure 1h). This pattern is more pronounced and located farther equatorward in winter than in summer (cf. supporting information Figures S1h and S3h). High AR frequencies extend from the subtropical western North Atlantic and Gulf of Mexico toward Western Europe (shading in Figure 1). Although AR frequencies of up to 40% in the North Atlantic in autumn might appear high, frequencies are lower in winter and compare well to other studies using relative thresholds along the European coasts (cf. AR frequency around 10% in winter in Figure S1h and Figure 9c in Guan & Waliser, 2015). It is striking that the maximum AR frequencies occur just to the southeast of the maximum gradient in Z500 reflecting the linkage of AR occurrence to the North Atlantic storm track. This agrees with the frequent location of ARs within the warm sector of extratropical cyclones (e.g., Bao et al., 2006; Dacre et al., 2015; Gimeno et al., 2014; Neiman et al., 2008; Ralph et al., 2004).

Autumn is used as exemplary season to describe the effect of WRs on ARs because (i) during the transition seasons, the seven different year-round WRs occur more evenly distributed than in summer or winter (e.g., only 3.5% of all summer days are in the zonal regime; Figure S3b) and (ii) the AR frequency is second largest in autumn (cf. Figures 1 and S1–S3 and Text S1). Our main conclusions hold for other seasons and with higher thresholds in the detection algorithm (see Supporting Information S1).

3.1. Modulation by WRs

The “Atlantic Trough” (AT), “Zonal” (ZO), and “Scandinavian Trough” (ScTr) regimes are dominated by negative 500-hPa geopotential height anomalies and enhanced extratropical cyclone activity (Grams et al., 2017; Papritz & Grams, 2018) and can thus be regarded as “cyclonic regimes.” The three regimes differ in the position of the accompanying upper-level trough. During the AT regime, the trough extends from Iceland toward Spain, and the gradient in Z500 is strongly enhanced compared to climatology (cf. contours in Figures 1a and 1h). This flow configuration doubles the probability of AR landfall at the northern coast of the Iberian Peninsula and the Atlantic coast of France and in southern England (cf. shading in Figures 1a and 1h) and facilitates a farther inland penetration of ARs. This is also reflected in the AR frequency anomaly which is strongly positive (up to >20 pp) over wide parts of western and central Europe (shading in Figure 2a).

The ZO regime also represents the positive phase of the NAO. Compared to AT, the trough is shifted westward and located farther to the North (contours in Figure 1b). This flow configuration favors AR landfall on the British Isles (shading in Figure 1b) with weakly (around 6 pp) enhanced AR frequency there and in the adjacent North Sea region (Figure 2b). During the ScTr regime, only a weak modulation of AR frequencies occurs over Europe (Figures 1c and 2c). However, ScTr is also accompanied by a weak ridge in the western North Atlantic which shifts AR activity further poleward there.

The ridge in the North Atlantic is even more amplified during the “Atlantic Ridge” (AtR) regime. Other “blocked regimes” that are characterized by a strong ridge and accompanying blocking anticyclone are the “European Blocking” (EuBL), “Scandinavian Blocking” (ScBL), and “Greenland Blocking” (GL) regimes.

During the AtR and EuBL regimes, the ridge extends from roughly 40°N to 60°N and over the North Atlantic and Europe, respectively (contours in Figures 1d and 1e). The Z500 gradient is enhanced around the ridge. As ARs in the western North Atlantic emerge at the southern flank of the storm track also at around 40°N, these flow configurations facilitate a steering of ARs around the ridge (contours in Figures 1d and 1e). Consequently, AR frequencies are enhanced at the western flanks of the ridge during AtR and EuBL regimes but strongly reduced in the center of the ridge (Figures 2d and 2e). During AtR, this modulation generally hinders AR landfall in Europe (reduction by up to 15 pp, Figure 2d) except for Iceland. During EuBL, however, the farther eastward location of the ridge allows for a more effective moisture transport around the ridge and into Northern Europe. Consequently, AR frequencies are enhanced (by around 9 pp) in a region extending from Iceland to Northern Scandinavia (Figure 2e).

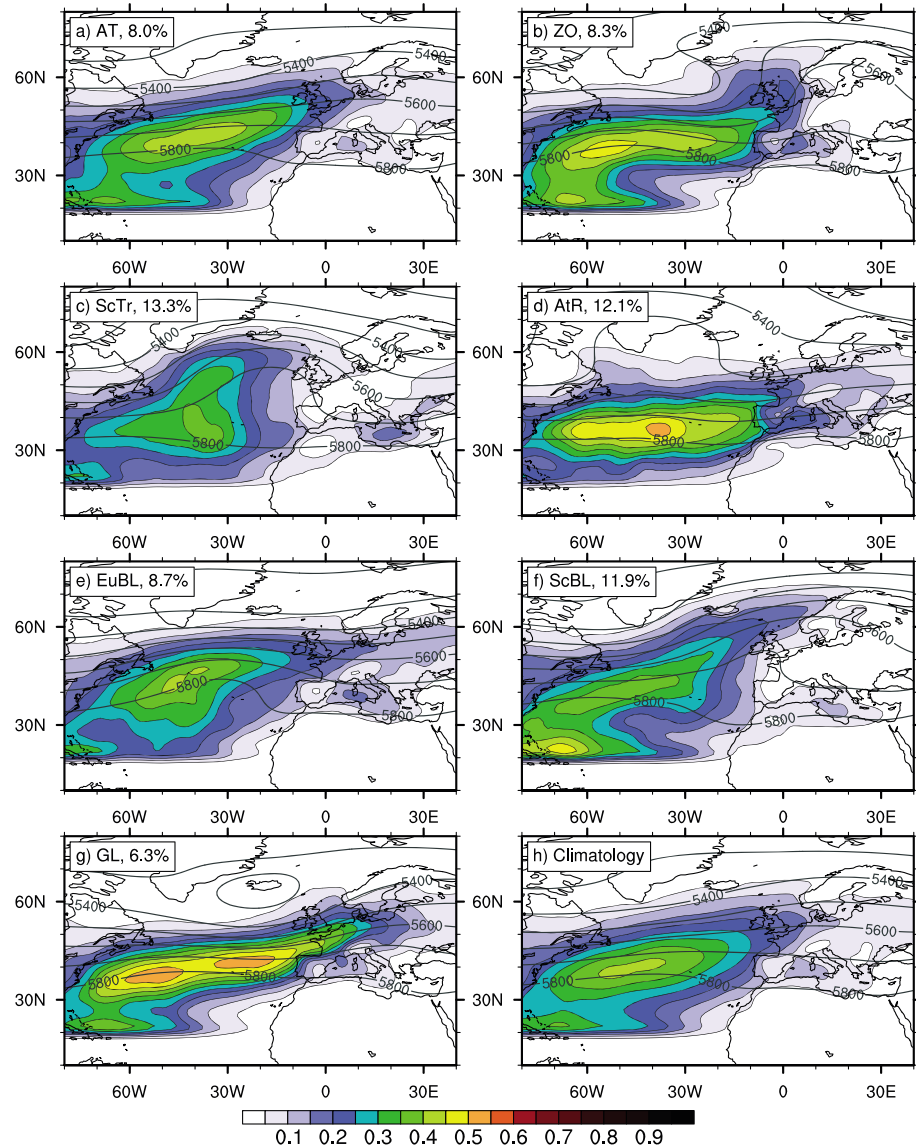


Figure 1. Atmospheric river frequency (shading, every 0.05 [5%] ranging from 0 to 1 [0–100%]) and Z500 (contours, every 100 gpm) in the North Atlantic region for all autumn (September to November) days attributed to one of the seven weather regimes (a–g) and climatology of Z500 and of atmospheric river frequency (h). Regime abbreviations and relative weather regime frequencies (for September to November, in percent) are indicated in the upper-left corner of each sub-panel. AT = Atlantic Trough; ZO = Zonal; ScTr = Scandinavian Trough; AtR = Atlantic Ridge; EuBL = European Blocking; ScBL = Scandinavian Blocking; GL = Greenland Blocking.

The ScBL and GL regimes are characterized by a blocking ridge at around 50–70°N over Scandinavia and Greenland, respectively. Due to the high latitude, these ridges go along with a southward shift of the jet stream and of cyclone activity. The meridional Z500 gradient is enhanced compared to climatology between 30°N and 50°N (cf. Figures 1f–1h). Consequently, also AR activity is focused into this zonal flow south of the blocking ridge (Figures 1f and 1, 2g) and AR frequencies are enhanced there (Figures 2f and 2g). During the GL regime, this results in a strongly increased likelihood of AR landfall on the Iberian Peninsula and in Morocco/North Africa (up to 18 pp; Figure 2g). At the same time, AR occurrence is reduced over the British Isles and in Scandinavia. During ScBL conditions, AR frequencies are enhanced over the Iberian Peninsula, but also weakly over the British Isles, due to a concomitant poleward deflection of AR activity on the western flank of the blocking ridge (Figure 2h).

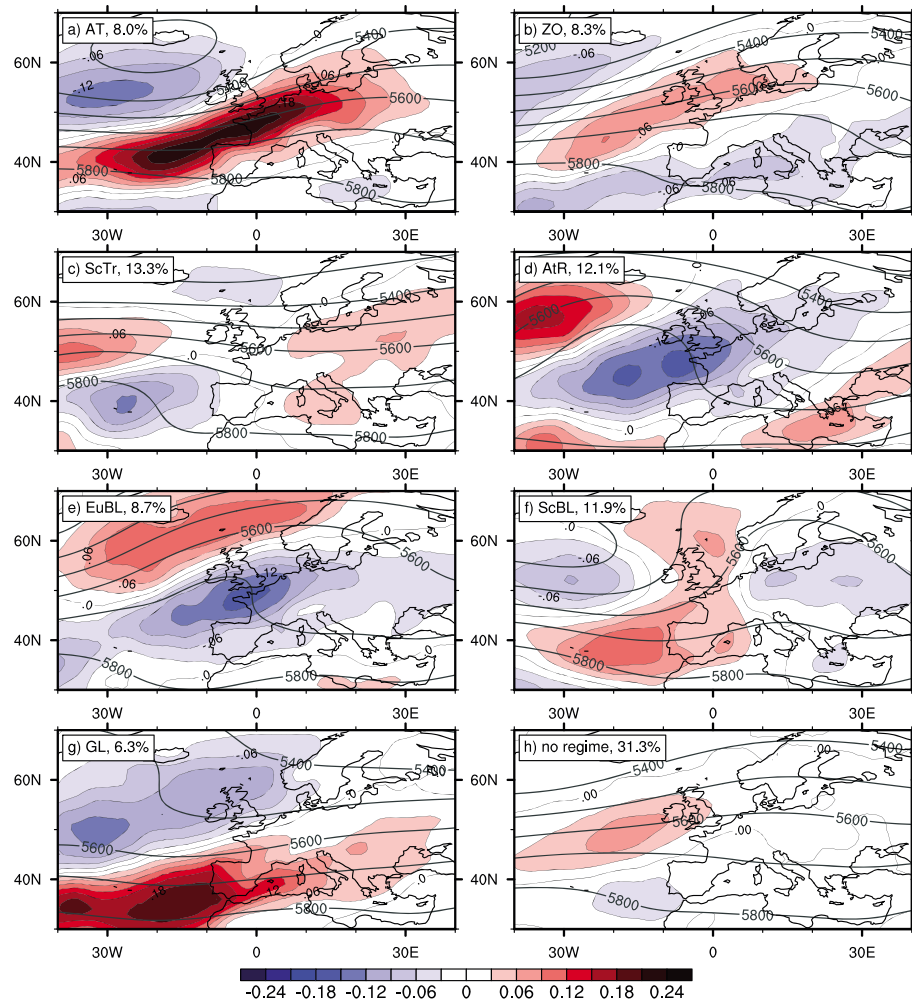


Figure 2. Atmospheric river frequency anomalies (shading, every 0.03 [3 percentage points]) and Z500 (contours, every 100 gpm) in the European region for all autumn (September to November) days attributed to one of the seven weather regimes (a–g) and to no regime (h). Regime abbreviations and relative weather regime frequencies (for September to November, in percent) are indicated in the upper-left corner of each subpanel. AT = Atlantic Trough; ZO = Zonal; ScTr = Scandinavian Trough; AtR = Atlantic Ridge; EuBL = European Blocking; ScBL = Scandinavian Blocking; GL = Greenland Blocking.

In summary, the investigation of AR frequencies during different WRs in autumn revealed that ARs are preferentially embedded into a region with an enhanced Z500 gradient and thus enhanced geostrophic flow. During cyclonic regimes such as the AT and ZO regimes, this enhanced gradient is primarily established by a negative Z500 anomaly and associated trough poleward of the mean westerly flow (Figure 1). During blocked regimes, the latitudinal position of the blocking ridge determines whether the mean westerly flow is predominantly deflected poleward, as during the AtR and EuBL regimes, or equatorward, as during the higher-latitude ScBL and GL regimes. The most striking modulation of AR activity occurs during the AT and the GL regimes with strongly enhanced AR landfall in western and central Europe and on the Iberian Peninsula and Northern Africa, respectively (Figure 2).

3.2. Enhanced Likelihood of PEs

Next, we explore the modulation of the occurrence of PEs during different WRs (Figure 3). Therefore, we compute at each grid point the fraction of 6-hourly time steps exceeding the 99th percentile of 6-hourly accumulated precipitation of the respective season at that grid point during the different regimes. If that fraction

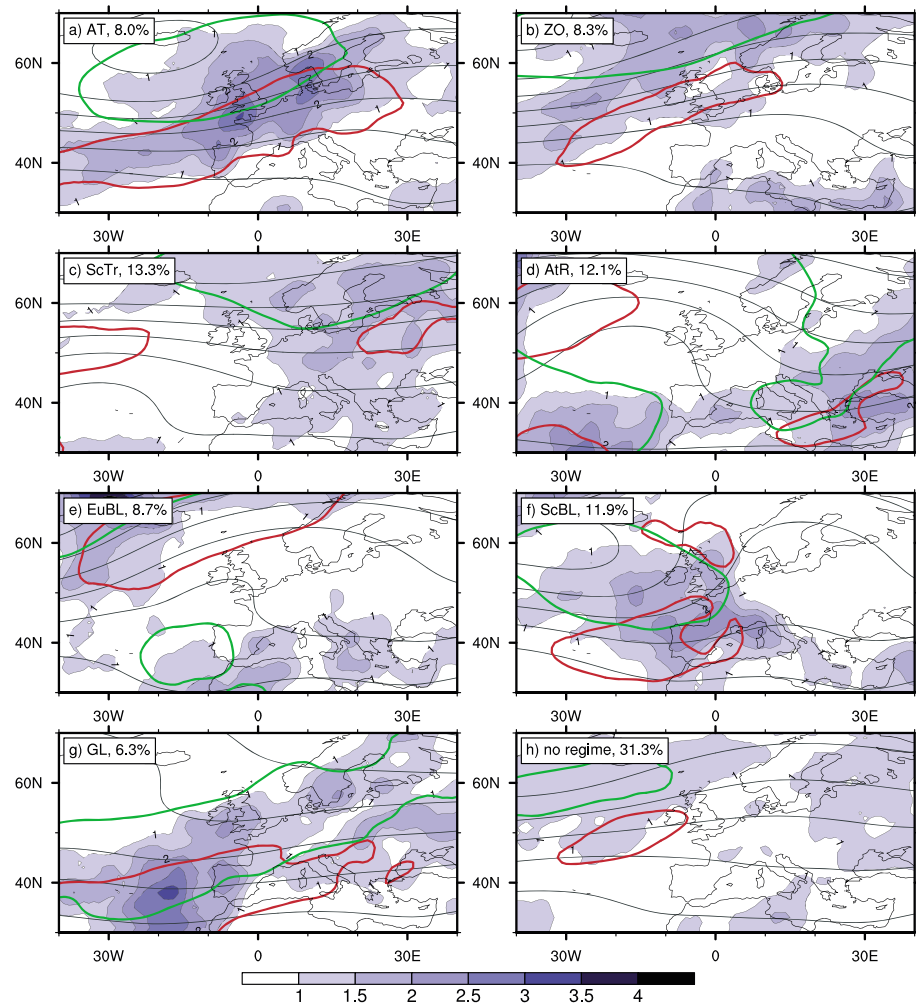


Figure 3. Enhanced frequency of precipitation extremes (PE; shading, every 0.5 ranging from 1 to 4) in the European region for all autumn (September to November) days attributed to one of the seven WRs (a–g) and to no regime (h). A value above 1.0 indicates that the relative PE frequency is higher than the seasonal mean, for example, 2.0 means that the relative PE frequency during the respective WR is double compared to the seasonal mean. Additional contours indicate 500-hPa geopotential height (black, every 100 gpm), positive atmospheric river frequency anomaly (red, 5% contour only), and positive cyclone frequency anomaly (green, 5% contour only). Regime abbreviations and relative WR frequencies (for September to November, in percent) are indicated in the upper-left corner of each sub-panel. AT = Atlantic Trough; ZO = Zonal; ScTr = Scandinavian Trough; AtR = Atlantic Ridge; EuBL = European Blocking; ScBL = Scandinavian Blocking; GL = Greenland Blocking.

is higher than 1%, the likelihood is enhanced (e.g., a fraction of 2% means a doubling of the likelihood of PEs at that grid point during the respective regime).

During the AT regime, the likelihood of a PE is strongly enhanced along the Atlantic, North Sea, and Baltic Sea coasts of Europe (Figure 3a). In Brittany, southern England, and around Denmark, the likelihood of a PE is 2.5 times higher during AT compared to the seasonal mean. The region of enhanced likelihood of a PE (Figure 3a) coincides with the region of enhanced AR activity during the AT regime (red contour in Figure 3a, cf. Figure 2a) suggesting that ARs help triggering the PEs. Indeed, in these regions, the AR frequency during a PE often exceeds 80% (Figure S7a). Further to the North, for example, over Ireland, Scotland, northern England, and Norway, the enhanced likelihood of PEs rather goes along with concomitant cyclone activity (green contour in Figure 3a; see also Pfahl & Wernli, 2012). During the ZO regime, the likelihood of PEs is enhanced over Northern Europe. Over the British Isles, PEs during ZO are also linked to AR activity (red contour in Figures 3b and S7b). However, the enhanced PE likelihood further to the north

and over Scandinavia is rather linked to cyclone activity (green contour in Figure 3b). Also during the ScTr regime, the enhanced likelihood of PEs over Scandinavia is related to enhanced cyclone activity (Figure 3c).

During the blocked AtR and EuBL regimes, PE are suppressed in wide parts of Europe (Figures 3d and 3e). However, during EuBL, enhanced PE likelihood co-occurs with AR activity in Iceland and northern Scandinavia (red contour in Figures 3e and S7e). In the central Mediterranean, the Balkans and west of Iberia enhanced likelihoods of PEs go along with enhanced cyclone activity during the AtR and EuBL regimes (green contours in Figures 3d and 3e) at the flanks of the blocking ridge. During AtR, the cyclone activity in the central Mediterranean might foster the formation of ARs in the eastern Mediterranean, which are more frequent in a region of twofold enhanced likelihood of PEs (red contour in Figure 3d).

The high-latitude blocked regimes ScBL and GL (Figures 3f and 3g) again enhance the likelihood of PEs across wider parts of Europe. During ScBL, most parts of Western Europe experience twofold more likely PEs than usual in autumn. Along the coasts of Iberia, southern France, Brittany, and Northern Scotland, the PEs often co-occur with AR activity (red contour in Figures 3f and S7f). At the same time, cyclone activity is enhanced over the British Isles (green contour in Figure 3f) at the upstream flank of the blocking ridge in regions of enhanced PE likelihood. During the GL regime, most parts of Europe experience a weakly enhanced likelihood of PEs except for the Alpine region and Eastern Europe (Figure 3g). Over parts of Iberia, North Africa/Morocco, the British Isles, and southern Sweden, the likelihood of PEs is twofold enhanced. While over Iberia, North Africa, and in the Mediterranean, these PEs occur in regions with enhanced AR activity (red contour in Figure 3g); in most parts of Europe, the enhanced PE likelihood occurs in regions of enhanced cyclone activity extending from the Azores Islands to the Baltic Sea (green contour in Figure 3g). Still, more than 80% of all PEs in Iberia, Morocco, and southern Ireland during GL co-occur with an AR (Figure S7g).

The investigation of the modulation of PE occurrence during different WRs revealed that indeed regions of enhanced AR activity also experience an enhanced likelihood of PEs. These PEs are then often associated with a concomitant AR. However, WRs also affect the occurrence of extratropical cyclones which can likewise trigger PEs. In particular at higher latitudes and further inland, an enhanced likelihood of PEs during different regimes therefore often goes along with enhanced cyclone activity.

4. Concluding Remarks

It has been extensively documented that (i) the large-scale flow in the North Atlantic-European region is modulated by the occurrence of specific WRs (e.g., Cassou, 2008; Grams et al., 2017; Michelangeli et al., 1995) and (ii) the large-scale moisture transport in ARs can be an important factor for the development of extreme precipitation events (e.g., Lavers & Villarini, 2013; Ralph et al., 2006; Ramos et al., 2015). In this study, we link these two aspects and provide a quantitative climatological analysis of the modulation of AR occurrence and the influence of AR on PEs by European WRs. We show that the spatial distribution of ARs, the probability of AR landfall in Europe, and, therefore, also the probability of European PEs are strongly modulated by the occurrence of different WRs. AR frequency is typically increased in regions of enhanced geostrophic wind velocities. In the UK, France, and northern Germany, AR landfall and associated PEs are strongly favored during the ZO and AT regimes. The probability of PEs thereby increases locally by more than 200%. The ScBL and GL regimes are associated with enhanced AR landfall and extreme precipitation over the Iberian Peninsula and the northwestern Mediterranean coast. These results broadly agree with previous studies showing an enhanced influence of ARs on precipitation over northern (southern) Europe during the positive (negative) phase of the NAO (Eiras-Barca et al., 2016; Lavers & Villarini, 2013; Stohl et al., 2008). Nevertheless, the WR approach adapted in this study provides a more detailed view on this modulation and explains a larger part of the flow variability compared to the NAO index.

To forecast the occurrence of high-impact PEs, in particular in coastal regions of Western Europe, it is thus crucial to take the effect of WRs into account. In turn, predictable variability of WRs on subseasonal time scales may provide opportunities to also forecast the probability of extreme precipitation beyond the classical weather prediction time scale of a few days, complementing current activities that started to explore and utilize the predictability of water vapor transport (Lavers, Pappenberger, et al., 2016; Lavers, Waliser, et al., 2016).

Acknowledgments

We thank two anonymous reviewers for their comments that helped improve the clarity of presenting our results. We are grateful to Heini Wernli, David Lavers, and Harald Sodemann for fruitful discussions on an early version of this study. We are very grateful to Heini Wernli and Peter Knippertz for providing us the AR data set. They originally compiled this data set for investigating the difference between atmospheric rivers, tropical moisture exports, and warm conveyor belts. This study will be published in the book “Atmospheric Rivers: Two Decades of Research”, edited by Ralph, M. F., Dettinger, M. D., Rutz, J. J., and Waliser, D. E. anticipated for 2019. The contribution of C. M. Grams was supported by the Swiss National Science Foundation (SNSF) grant PZ00P2_148177/1 and completed while he holds a Young Investigator Group grant by the German Helmholtz Association (VH-NG-1243). We acknowledge ECMWF for providing the ERA-Interim reanalysis data set available from <http://www.ecmwf.int>. Derived quantities are available through the methodologies described and referenced in section 2.

References

- Bao, J.-W., Michelson, S. A., Neiman, P. J., Ralph, F. M., & Wilczak, J. M. (2006). Interpretation of enhanced integrated water vapor bands associated with extratropical cyclones: Their formation and connection to tropical moisture. *Monthly Weather Review*, *134*(4), 1063–1080. <https://doi.org/10.1175/MWR3123.1>
- Blamey, R. C., Ramos, A. M., Trigo, R. M., Tomé, R., & Reason, C. J. C. (2018). The influence of atmospheric rivers over the South Atlantic on winter rainfall in South Africa. *Journal of Hydrometeorology*, *19*(1), 127–142. <https://doi.org/10.1175/JHM-D-17-0111.1>
- Brands, S., Gutiérrez, J. M., & San-Martín, D. (2017). Twentieth-century atmospheric river activity along the west coasts of Europe and North America: Algorithm formulation, reanalysis uncertainty and links to atmospheric circulation patterns. *Climate Dynamics*, *48*(9–10), 2771–2795. <https://doi.org/10.1007/s00382-016-3095-6>
- Cassou, C. (2008). Intraseasonal interaction between the Madden-Julian Oscillation and the North Atlantic Oscillation, supplementary method. *Nature*, *455*(7212), 523–527. <https://doi.org/10.1038/nature07286>
- Champion, A. J., Allan, R. P., & Lavers, D. A. (2015). Atmospheric rivers do not explain UK summer extreme rainfall. *Journal of Geophysical Research: Atmospheres*, *120*, 6731–6741. <https://doi.org/10.1002/2014JD022863>
- Dacre, H. F., Clark, P. A., Martínez-Alvarado, O., Stringer, M. A., & Lavers, D. A. (2015). How do atmospheric rivers form? *Bulletin of the American Meteorological Society*, *96*(8), 1243–1255. <https://doi.org/10.1175/BAMS-D-14-00031.1>
- Dee, D. P., Uppala, S. M., Simmons, A. J., Berrisford, P., Poli, P., Kobayashi, S., et al. (2011). The ERA-Interim reanalysis: Configuration and performance of the data assimilation system. *Quarterly Journal of the Royal Meteorological Society*, *137*(656), 553–597. <https://doi.org/10.1002/qj.828>
- Dettinger, M. D. (2011). Climate change, atmospheric rivers, and floods in California—A multimodel analysis of storm frequency and magnitude changes. *Journal of the American Water Resources Association*, *47*(3), 514–523. <https://doi.org/10.1111/j.1752-1688.2011.00546.x>
- Dettinger, M. D., Ralph, F. M., Das, T., Neiman, P. J., & Caya, D. R. (2011). Atmospheric Rivers, Floods and the Water Resources of California. *Water*, *3*(2), 445–478. <https://doi.org/10.3390/w3020445>
- Eiras-Barca, J., Brands, S., & Miguez-Macho, G. (2016). Seasonal variations in North Atlantic atmospheric river activity and associations with anomalous precipitation over the Iberian Atlantic margin. *Journal of Geophysical Research: Atmospheres*, *121*, 931–948. <https://doi.org/10.1002/2015JD023379>
- Ferranti, L., Corti, S., & Janousek, M. (2015). Flow-dependent verification of the ECMWF ensemble over the Euro-Atlantic sector. *Quarterly Journal of the Royal Meteorological Society*, *141*(688), 916–924. <https://doi.org/10.1002/qj.2411>
- Gershunov, A., Shulgina, T., Ralph, F. M., Lavers, D. A., & Rutz, J. J. (2017). Assessing the climate-scale variability of atmospheric rivers affecting western North America. *Geophysical Research Letters*, *44*, 7900–7908. <https://doi.org/10.1002/2017GL074175>
- Gimeno, L., Nieto, R., Vázquez, M., & Lavers, D. (2014). Atmospheric rivers: A mini-review. *Frontiers in Earth Science*, *2*, 2. <https://doi.org/10.3389/feart.2014.00002>
- Gorodetskaya, I. V., Tsukernik, M., Claes, K., Ralph, M. F., Neff, W. D., & Van Lipzig, N. P. M. (2014). The role of atmospheric rivers in anomalous snow accumulation in East Antarctica. *Geophysical Research Letters*, *41*, 6199–6206. <https://doi.org/10.1002/2014GL060881>
- Grams, C. M., Beerli, R., Pfenninger, S., Staffell, I., & Wernli, H. (2017). Balancing Europe's wind-power output through spatial deployment informed by weather regimes. *Nature Climate Change*, *7*(8), 557–562. <https://doi.org/10.1038/nclimate3338>
- Guan, B., Molotch, N. P., Waliser, D. E., Fetzer, E. J., & Neiman, P. J. (2010). Extreme snowfall events linked to atmospheric rivers and surface air temperature via satellite measurements. *Geophysical Research Letters*, *37*, L20401. <https://doi.org/10.1029/2010GL044696>
- Guan, B., & Waliser, D. E. (2015). Detection of atmospheric rivers: Evaluation and application of an algorithm for global studies. *Journal of Geophysical Research: Atmospheres*, *120*, 12,514–12,535. <https://doi.org/10.1002/2015JD024257>
- Hirota, N., Takayabu, Y. N., Kato, M., & Arakane, S. (2016). Roles of an atmospheric river and a cutoff low in the extreme precipitation event in Hiroshima on 19 August 2014. *Monthly Weather Review*, *144*(3), 1145–1160. <https://doi.org/10.1175/MWR-D-15-0299.1>
- Jankov, I., Bao, J.-W., Neiman, P. J., Schultz, P. J., Yuan, H., & White, A. B. (2009). Evaluation and comparison of microphysical algorithms in ARW-WRF model simulations of atmospheric river events affecting the California coast. *Journal of Hydrometeorology*, *10*(4), 847–870. <https://doi.org/10.1175/2009JHM1059.1>
- Knippertz, P., & Wernli, H. (2010). A lagrangian climatology of tropical moisture exports to the northern hemispheric extratropics. *Journal of Climate*, *23*(4), 987–1003. <https://doi.org/10.1175/2009JCLI3333.1>
- Lavers, D. A., Allan, R. P., Villarini, G., Lloyd-Hughes, B., Brayshaw, D. J., & Wade, A. J. (2013). Future changes in atmospheric rivers and their implications for winter flooding in Britain. *Environmental Research Letters*, *8*(3), 034010. <https://doi.org/10.1088/1748-9326/8/3/034010>
- Lavers, D. A., Allan, R. P., Wood, E. F., Villarini, G., Brayshaw, D. J., & Wade, A. J. (2011). Winter floods in Britain are connected to atmospheric rivers. *Geophysical Research Letters*, *38*, L23803. <https://doi.org/10.1029/2011GL049783>
- Lavers, D. A., Pappenberger, F., Richardson, D. S., & Zsoter, E. (2016). ECMWF Extreme Forecast Index for water vapor transport: A forecast tool for atmospheric rivers and extreme precipitation. *Geophysical Research Letters*, *43*, 11,852–11,858. <https://doi.org/10.1002/2016GL071320>
- Lavers, D. A., & Villarini, G. (2013). The nexus between atmospheric rivers and extreme precipitation across Europe. *Geophysical Research Letters*, *40*, 3259–3264. <https://doi.org/10.1002/grl.50636>
- Lavers, D. A., Villarini, G., Allan, R. P., Wood, E. F., & Wade, A. J. (2012). The detection of atmospheric rivers in atmospheric reanalyses and their links to British winter floods and the large-scale climatic circulation. *Journal of Geophysical Research*, *117*, D20106. <https://doi.org/10.1029/2012JD018027>
- Lavers, D. A., Waliser, D. E., Ralph, F. M., & Dettinger, M. D. (2016). Predictability of horizontal water vapor transport relative to precipitation: Enhancing situational awareness for forecasting western U.S. extreme precipitation and flooding. *Geophysical Research Letters*, *43*, 2275–2282. <https://doi.org/10.1002/2016GL067765>
- Madonna, E., Li, C., Grams, C. M., & Woollings, T. (2017). The link between eddy-driven jet variability and weather regimes in the North Atlantic-European sector. *Quarterly Journal of the Royal Meteorological Society*, *143*(708), 2960–2972. <https://doi.org/10.1002/qj.3155>
- Mastin, M. C., Grendaszek, A. S., & Barnas, C. R. (2010). Magnitude and extent of flooding at selected river reaches in western Washington, January 2009: USGS Scientific Investigations Report 2010–5177 (34 pp). Reston, VA: U.S. Geological Survey. Retrieved from <https://pubs.usgs.gov/sir/2010/5177/pdf/sir20105177.pdf>
- Michelangeli, P.-A., Vautard, R., & Legras, B. (1995). Weather regimes: Recurrence and quasi stationarity. *Journal of the Atmospheric Sciences*, *52*(8), 1237–1256. [https://doi.org/10.1175/1520-0469\(1995\)052<1237:WRRASQ>2.0.CO;2](https://doi.org/10.1175/1520-0469(1995)052<1237:WRRASQ>2.0.CO;2)

- Moore, B. J., Neiman, P. J., Ralph, F. M., & Barthold, F. E. (2012). Physical processes associated with heavy flooding rainfall in Nashville, Tennessee, and vicinity during 1–2 May 2010: The role of an atmospheric river and mesoscale convective systems. *Monthly Weather Review*, *140*(2), 358–378. <https://doi.org/10.1175/MWR-D-11-00126.1>
- Neiman, P. J., Ralph, F. M., Moore, B. J., Hughes, M., Mahoney, K. M., Cordeira, J. M., & Dettinger, M. D. (2013). The landfall and inland penetration of a flood-producing atmospheric river in Arizona. Part I: Observed synoptic-scale, orographic, and hydrometeorological characteristics. *Journal of Hydrometeorology*, *14*(2), 460–484. <https://doi.org/10.1175/JHM-D-12-0101.1>
- Neiman, P. J., Ralph, F. M., Wick, G. A., Lundquist, J. D., & Dettinger, M. D. (2008). Meteorological characteristics and overland precipitation impacts of atmospheric rivers affecting the west coast of North America based on eight years of SSM/I satellite observations. *Journal of Hydrometeorology*, *9*(1), 22–47. <https://doi.org/10.1175/2007JHM855.1>
- Neiman, P. J., Schick, L. J., Ralph, F. M., Hughes, M., & Wick, G. A. (2011). Flooding in western Washington: The connection to atmospheric rivers. *Journal of Hydrometeorology*, *12*(6), 1337–1358. <https://doi.org/10.1175/2011JHM1358.1>
- Papritz, L., & Grams, C. M. (2018). Linking low-frequency large-scale circulation patterns to cold air outbreak formation in the north-eastern North Atlantic. *Geophysical Research Letters*, *45*, 2542–2553. <https://doi.org/10.1002/2017GL076921>
- Payne, A. E., & Magnusdottir, G. (2014). Dynamics of landfalling atmospheric rivers over the North Pacific in 30 years of MERRA reanalysis. *Journal of Climate*, *27*(18), 7133–7150. <https://doi.org/10.1175/JCLI-D-14-00034.1>
- Pfahl, S., & Wernli, H. (2012). Quantifying the relevance of cyclones for precipitation extremes. *Journal of Climate*, *25*(19), 6770–6780. <https://doi.org/10.1175/JCLI-D-11-00705.1>
- Piaget, N., Froidevaux, P., Giannakaki, P., Gierth, F., Martius, O., Riemer, M., et al. (2015). Dynamics of a local alpine flooding event in October 2011: Moisture source and large-scale circulation. *Quarterly Journal of the Royal Meteorological Society*, *141*(690), 1922–1937. <https://doi.org/10.1002/qj.2496>
- Ralph, F. M., & Dettinger, M. D. (2011). Storms, floods, and the science of atmospheric rivers. *Eos, Transactions of the American Geophysical Union*, *92*(32), 265–266. <https://doi.org/10.1029/2011EO320001>
- Ralph, F. M., Neiman, P. J., & Rotunno, R. (2005). Dropsonde observations in low-level jets over the Northeastern Pacific Ocean from CALJET-1998 and PACJET-2001: Mean vertical-profile and atmospheric-river characteristics. *Monthly Weather Review*, *133*(4), 889–910. <https://doi.org/10.1175/MWR2896.1>
- Ralph, F. M., Neiman, P. J., & Wick, G. A. (2004). Satellite and CALJET aircraft observations of atmospheric rivers over the eastern North Pacific Ocean during the winter of 1997/98. *Monthly Weather Review*, *132*(7), 1721–1745. [https://doi.org/10.1175/1520-0493\(2004\)132<1721:SACAOO>2.0.CO;2](https://doi.org/10.1175/1520-0493(2004)132<1721:SACAOO>2.0.CO;2)
- Ralph, F. M., Neiman, P. J., Wick, G. A., Gutman, S. I., Dettinger, M. D., Cayan, D. R., & White, A. B. (2006). Flooding on California's Russian River: Role of atmospheric rivers. *Geophysical Research Letters*, *33*, L13801. <https://doi.org/10.1029/2006GL026689>
- Ramos, A. M., Trigo, R. M., Liberato, M. L. R., & Tomé, R. (2015). Daily precipitation extreme events in the Iberian Peninsula and its association with atmospheric rivers. *Journal of Hydrometeorology*, *16*(2), 579–597. <https://doi.org/10.1175/JHM-D-14-0103.1>
- Rivera, E. R., Dominguez, F., & Castro, C. L. (2014). Atmospheric rivers and cool season extreme precipitation events in the Verde River basin of Arizona. *Journal of Hydrometeorology*, *15*(2), 813–829. <https://doi.org/10.1175/JHM-D-12-0189.1>
- Rutz, J. J., Steenburgh, W. J., & Ralph, F. M. (2014). Climatological characteristics of atmospheric rivers and their inland penetration over the western United States. *Monthly Weather Review*, *142*(2), 905–921. <https://doi.org/10.1175/MWR-D-13-00168.1>
- Santos, J. A., Belo-Pereira, M., Fraga, H., & Pinto, J. G. (2016). Understanding climate change projections for precipitation over Western Europe with a weather typing approach. *Journal of Geophysical Research: Atmospheres*, *121*, 1170–1189. <https://doi.org/10.1002/2015JD024399>
- Shields, C. A., Rutz, J. J., Leung, L.-Y., Ralph, F. M., Wehner, M., Kawzenuk, B., et al. (2018). Atmospheric River Tracking Method Intercomparison Project (ARTMIP): Project goals and experimental design. *Geoscience Model Development*, *11*(6), 2455–2474. <https://doi.org/10.5194/gmd-11-2455-2018>
- Sodemann, H., & Stohl, A. (2013). Moisture origin and meridional transport in atmospheric rivers and their association with multiple cyclones. *Monthly Weather Review*, *141*(8), 2850–2868. <https://doi.org/10.1175/MWR-D-12-00256.1>
- Sprenger, M., Fragkoulidis, G., Binder, H., Croci-Maspoli, M., Graf, P., Grams, C. M., et al. (2017). Global Climatologies of Eulerian and Lagrangian flow features based on ERA-Interim. *Bulletin of the American Meteorological Society*, *98*(8), 1739–1748. <https://doi.org/10.1175/BAMS-D-15-00299.1>
- Stohl, A., Forster, C., & Sodemann, H. (2008). Remote sources of water vapor forming precipitation on the Norwegian west coast at 60° N—A tale of hurricanes and an atmospheric river. *Journal of Geophysical Research*, *113*, D05102. <https://doi.org/10.1029/2007JD009006>
- Viale, M., & Nuñez, M. N. (2011). Climatology of winter orographic precipitation over the subtropical Central Andes and associated synoptic and regional characteristics. *Journal of Hydrometeorology*, *12*(4), 481–507. <https://doi.org/10.1175/2010JHM1284.1>
- Warner, M. D., Mass, C. F., & Salathé, E. P. (2015). Changes in winter atmospheric rivers along the North American West Coast in CMIP5 climate models. *Journal of Hydrometeorology*, *16*(1), 118–128. <https://doi.org/10.1175/JHM-D-14-0080.1>
- Wernli, H., & Schwierz, C. (2006). Surface cyclones in the era-40 dataset (1958–2001). Part I: Novel identification method and global climatology. *Journal of the Atmospheric Sciences*, *63*(10), 2486–2507. <https://doi.org/10.1175/JAS3766.1>
- Yiou, P., & Nogaj, M. (2004). Extreme climatic events and weather regimes over the North Atlantic: When and where? *Geophysical Research Letters*, *31*, L07202. <https://doi.org/10.1029/2003GL019119>
- Zhu, Y., & Newell, R. E. (1998). A proposed algorithm for moisture fluxes from atmospheric rivers. *Monthly Weather Review*, *126*(3), 725–735. [https://doi.org/10.1175/1520-0493\(1998\)126<0725:APAFMF>2.0.CO;2](https://doi.org/10.1175/1520-0493(1998)126<0725:APAFMF>2.0.CO;2)
- Zubiate, L., McDermott, F., Sweeney, C., & O'Malley, M. (2017). Spatial variability in winter NAO–wind speed relationships in Western Europe linked to concomitant states of the East Atlantic and Scandinavian patterns. *Quarterly Journal of the Royal Meteorological Society*, *143*(702), 552–562. <https://doi.org/10.1002/qj.2943>